

EFFECT OF TIN PRECURSORS ON THE DEPOSITION OF $\text{Cu}_2\text{ZnSnS}_4$ THIN FILMS

D. NAGAMALLESWARI^{a,b}, Y. B. KISHOREKUMAR^{a,*}, Y. B. KIRAN^c,
G. SURESHBABU^d

^a*Solar Energy Laboratory, Sree Vidyanikethan Engineering College, Tirupati, India*

^b*Department of Physics, Jawaharlal Nehru Technological University Ananthapur, Anantapuramu, India*

^c*Center for Applied Sciences, Sree Vidyanikethan Engineering College, Tirupati, India*

^d*Department of Physics, Government Degree College, Pakala, India*

$\text{Cu}_2\text{ZnSnS}_4$ is a potential compound semiconducting material for solar absorber layer in thin film heterojunction solar cells. Chemical spray pyrolysis technique has been successfully employed to deposit these thin films using two different tin precursors. Thin films were characterized by studying their structural, composition, electrical and optical properties. X-ray diffraction pattern reveals that these films exhibit polycrystalline nature with kesterite structure. Lattice parameters of $\text{Cu}_2\text{ZnSnS}_4$ films are found to be $a = b = 0.544$ nm and $c = 1.084$ nm. Optical band gap, evaluated from spectral transmittance data, is close to ideal energy gap (1.5 eV) exhibit highest conversion efficiency. Optical absorption coefficient of these films is $\geq 10^4$ cm^{-1} . These films exhibit p-type nature. A humble attempt is made to fabricate a typical heterojunction $\text{Cu}_2\text{ZnSnS}_4$ thin film solar cell.

(Received June 25, 2020; Accepted October 8, 2020)

Keywords: $\text{Cu}_2\text{ZnSnS}_4$, Thin films, Absorber layer, Chemical spray technique, Structural properties, Solar cell

1. Introduction

With the rapid growth in population, a rush in urbanization and industrialization, the usage of electricity increased and the affordable electric power also increased. At present the usual power consumption is about 10 TW and it is projected around 30 TW by 2050 [1]. Unfortunately, the energy assets are meager. In the next few decades, the existing fossil fuels in the world are going to drain out. Hence world is looking towards the renewable energy sources. In this contest, for the tropical countries solar energy is one of the best potential renewable energy sources.

In recent years, photovoltaic investigations have been directed towards ternary and quaternary chalcopyrite semiconductors like CuInSe_2 , CuGaSe_2 , $\text{Cu}(\text{In,Ga})(\text{S,Se})_2$ (CIGS), and CuInSSe_2 . Thin films heterojunction solar cells based on CIGS with an efficiency of about 22.9% on a small area have been realized [2]. However, the elements indium and gallium are scarce and expensive. In order to attain the commercial solar cells, researchers are needed to work on suitable alternative materials and techniques. In this context, $\text{Cu}_2\text{ZnSnS}_4$ (CZTS) is an alternative absorber layer to CIGS thin films due to its non-toxic and environmentally friendly nature. Hence CZTS is considered to be a potential absorber material [3]. CZTS films have salient properties such as direct band gap nature (1.45 eV), exhibiting high absorption coefficient ($\geq 10^4$ cm^{-1}), tetragonal structure and p-type in nature [4]. The elements in these absorber layers are available abundantly at low cost. Hence there is a possibility to grow inexpensive thin film solar cells. In 2018, Chang et al. reported 11% as maximum conversion efficiency of CZTS thin film solar cells [5]. In order to progress the conversion efficiency and make CZTS industrial viable, a lot of research is still

* Corresponding author: ybkksvu@gmail.com

necessary. Several researchers have been working on this material and successfully developed using various physical as well as chemical techniques. CZTS thin films have been successfully deposited by magnetron sputtering [6], co-evaporation [7], electron beam evaporation [8], Thermal evaporation [9], pulsed laser deposition [10], electro deposition [11, 12], SILAR [13], sol-gel [14], chemical bath deposition [15], and chemical spray pyrolysis [16, 17] methods. Among these, chemical spray pyrolysis is one of the trouble-free, economical and versatile techniques for the deposition sulphide and oxide films [18].

This chemical method is used in the present investigation to deposit CZTS thin films. Films were characterized using structural, optical, composition and electrical properties of CZTS thin films deposited with two different tin salt precursors. Finally, an effort is made for fabrication of $\text{Cu}_2\text{ZnSnS}_4$ thin film solar cell.

2. Experimental method

CZTS films were deposited using indigenously fabricated chemical spray pyrolysis system. Ultrasonically and chemically cleaned soda-lime glass substrates were kept on stainless steel hot plate. Films were deposited at optimized temperature which is 643 K with a precision of ± 5 K [19]. This is achieved with the help of high temperature digital controller. The spray nozzle (Model: $\frac{1}{4}$ JAU, M/S Spraying Systems Company) and electrical heater assembly were kept surrounded by a fume cupboard attached with an exhaust duct & fan for eradicating gas fumes and hot vapors of the solvent. The front side of cupboard is fixed with movable glass doors which were kept closed during the pyrolysis. The distance between spray nozzle and substrate was kept around 30 cm for optimum coverage of droplet cone on the substrates. The additional supplementary deposition conditions like carrier gas pressure, solution spray rate was maintained as 3.0 kg/cm^2 and 15 ml/min respectively. Compressed air was used to atomize the spray solution.

In the present study, salts of stannous chloride and stannic chloride were used as tin precursors. Films were deposited with a freshly prepared aqueous solution containing salts of cupric chloride, zinc acetate, stannous / stannic chloride and thiourea in the molar ratio 1.8:1:1:10 [20]. Due to volatile nature of sulphur, the molarity of sulphur source was taken more than stoichiometry requirement to reimburse the loss of sulphur during experiment. Films deposited using aqueous solutions consisting of stannous chloride were named as 'A' and those with stannic chloride as 'B'. The pH of the precursor solutions was ~ 2.9 and 3.4. For dissolving stannous chloride salts, small drops of dilute hydrochloric acid are added to the aqueous solution.

After successfully spray pyrolysis, these films were annealed at (T_a) 760 K in sulphur atmosphere using the two-zone tubular quartz furnace. While as deposited films were kept in primary hot zone of the tubular furnace, Sigma-Aldrich make sulphur pellets (99.998%) were kept gently in to the other hot zone of the furnace placing in a molybdenum boat. The temperature of two zones in tubular furnace could be controlled with the help of PID controllers. One end of tubular furnace was closed with SS end connector and the other end is connected to a rotary pump attached with a pirani gauge. Inside the furnace a steady working pressure was maintained by using rotary pump. After achieving the desired pressure, temperature of primary hot zone was slowly increased with temperature controller at the rate of 10 K/min. During annealing process, secondary hot zone (sulphur source) was kept under constant evaporation to compensate the loss of sulphur from the films. Under these conditions' films were annealed for about 60 minutes. After the successful completion of annealing in sulphur atmosphere, the temperature of hot zones was cooled to 390 K at the rate of 6 K/min and finally allowed them to cool naturally.

The structural characteristics of these films were analyzed with the help of Powder X-ray diffractometer (XRD) and micro Raman spectra. The XRD patterns of these films were recorded using $\text{Cu K}\alpha$ radiation ($\lambda = 0.15406 \text{ nm}$) with BRUKER computer-controlled X-ray diffractometer. micro Raman spectra of these films were recorded in the back-scattering mode using Argon ion laser source of wavelength 514.3 nm. The elemental content of these films were measured using energy dispersive spectrometer (EDS). The JEOL scanning electron microscope (SEM) was used to study the surface morphology of CZTS films. Spectral transmittance of the films was recorded

with UV-Vis-NIR double beam spectrophotometer (JASCO). The electrical parameters of these films were determined using the Hall Effect as well as van der Pauw techniques.

3. Results and discussion

The CZTS films deposited using by chemical spray pyrolysis technique are extremely adherent to the substrates and uniform in nature.

Table 1 contains of the comprehensive chemical composition of spray deposited and annealed $\text{Cu}_2\text{ZnSnS}_4$ films using two tin precursors (A & B). First two lines in Table 1 show the elemental composition of CZTS films deposited with solution A. The EDS analysis reveals that as deposited CZTS films are sulphur poor. On annealing there is significant improvement in sulphur and Zinc. The next two lines in Table 1 represent the chemical composition of CZTS films deposited with solution B. As deposited CZTS films were slightly poor in Cu, S and Zn-rich. On annealing these samples, there is significant improvement in sulphur composition. A minute change was observed in the chemical composition of rest of the elements present in the film. On annealing, in both the precursors' tin composition was slightly decreased. Cu-poor and Zn-rich conditions are highly favorable for efficient CZTS thin films solar cells [8, 21].

Table 1. Elemental composition of CZTS films.

Sample Code	Condition	Cu (at.%)	Zn (at.%)	Sn (at.%)	S (at.%)	Cu/(Zn+Sn)	Zn/Sn	S/met al
A	As deposited	29.8	14.8	13.6	41.8	1.049	1.088	0.718
	Annealed at 760 K	28.4	14.6	12.7	44.3	1.040	1.150	0.795
B	As deposited	26.1	16.1	13.3	44.5	0.888	1.211	0.802
	Annealed at 760 K	25.8	15.9	12.6	45.7	0.905	1.262	0.842

Fig. 1 shows the powder XRD pattern of chemical spray deposited CZTS films with two tin precursors (A & B). The XRD analysis reveals that the crystalline films orientated along (112) plane exhibiting polycrystalline nature with kesterite structure [22] and close agreement with JCPDS card No. 26-0575. The films deposited with an aqueous solution consisting stannous chloride were found to contain Cu_{2-x}S [42-0564], and Cu_2SnS_3 (CTS) [89-4714] as secondary phases along with characteristics peaks of CZTS. The films deposited with solution having of salts of stannic chloride exhibits low intense peaks corresponding to the (220)/(204), (312)/(116) and (224) planes of CZTS along with (112) plane. However, the substantial aberrations in the composition of CZTS films indicates the occurrence of either binaries or ternaries might be exists in amorphous phases.

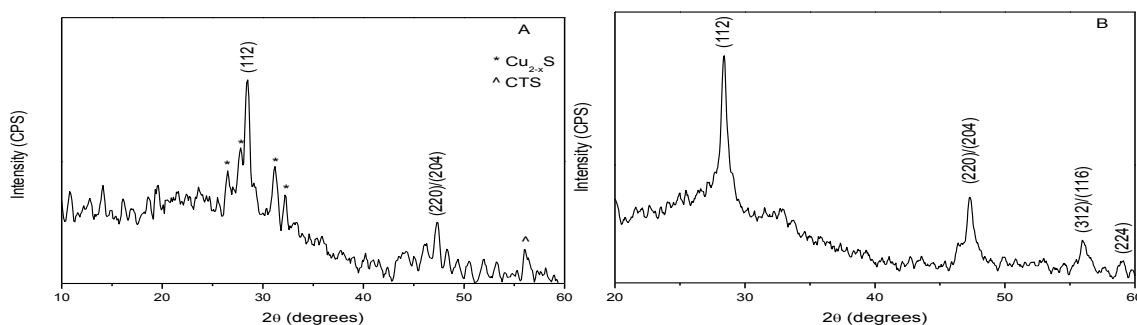


Fig. 1. XRD pattern of spray deposited CZTS films with two tin precursors (A & B).

The XRD pattern of CZTS films deposited with two tin precursors which are annealed in sulphur ambiance at 760 K were shown in Fig. 2. On annealing, significant improvement was

obtained in the intensity of peaks. The decline in peak width on annealing in sulphur atmosphere indicates a significant progress in crystallite size. On annealing, intensity ratio of (112) to (220) XRD peaks was increased significantly. In case of the films deposited with stannous chloride solution, Cu_{2-x}S peak intensity was increased with (220)/(204) peak of CZTS.

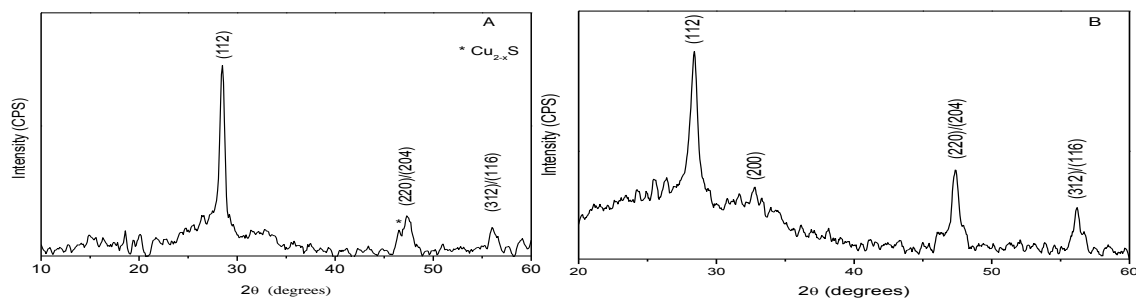


Fig. 2. XRD pattern of CZTS films with two tin precursors (A & B) annealed at 760 K.

The lattice parameters of tetragonal structure (kesterite) can be obtained from d-spacings using the following equation [23]

$$d_{hkl} = \frac{a}{\sqrt{h^2 + k^2 + l^2}}$$

here d_{hkl} is inter planar distance corresponding to (hkl) plane. The lattice parameters of these films are found to be $a = b = 0.544$ nm and $c = 1.084$ nm respectively. The obtained values are in concord with the standard data card No. 26-0575 and reported values [22, 24]. The broad peak indicates that the grain size is extremely small. The crystallite size (L) of these films were calculated from the (112) peak of CZTS using the Debye-Scherrer's equation $L = K\lambda / \beta \cos\theta$ where K is constant (0.9), λ is the wavelength of X-ray radiation were used, β is Full Width at Half Maximum (FWHM) and θ is diffraction angle of the corresponding peak [23]. The mean crystallite sizes of CZTS films with two tin precursors were found to be 26 and 15 nm correspondingly. The number of grains per unit area in the films were obtained using a simple relation $N = t/L^3$ where t is the thickness of the film and L is crystallite size [25]. The number of grains per unit area was found to be 2.8×10^{16} and $1.04 \times 10^{17} \text{ cm}^{-2}$ for the two tin precursors A and B respectively. The number of grains per unit area was found to increase when the films were grown by the aqueous solution containing salts of stannic chloride.

Raman spectroscopy is a powerful tool to recognize the phase and structure analysis of compounds. The micro-Raman spectrum of spray deposited CZTS films with two different tin precursors were shown in Fig. 3. The Raman modes occurred at 289, 329, 339, 349 and 475 cm^{-1} respectively for the films deposited with the solution A. The Raman peaks at 289 cm^{-1} , 339 cm^{-1} and shoulder peak at 349 cm^{-1} were attributed to CZTS [26]. The limb peak at 329 cm^{-1} and minor peak at 475 cm^{-1} were ascribed to tetragonal CTS [27] and Cu_{2-x}S [26]. The same trend was observed in the XRD analysis. The films deposited with stannic chloride salt solution (B) exhibits the Raman modes at 316, 339, and 371 cm^{-1} subsequently. The intense Raman mode at 339 cm^{-1} and mode at 371 cm^{-1} indicate the existence of the CZTS in the sample [26]. The low intense Raman mode at 316 cm^{-1} indicates the existence of the secondary phase in the film and it is ascribed to SnS_2 [26].

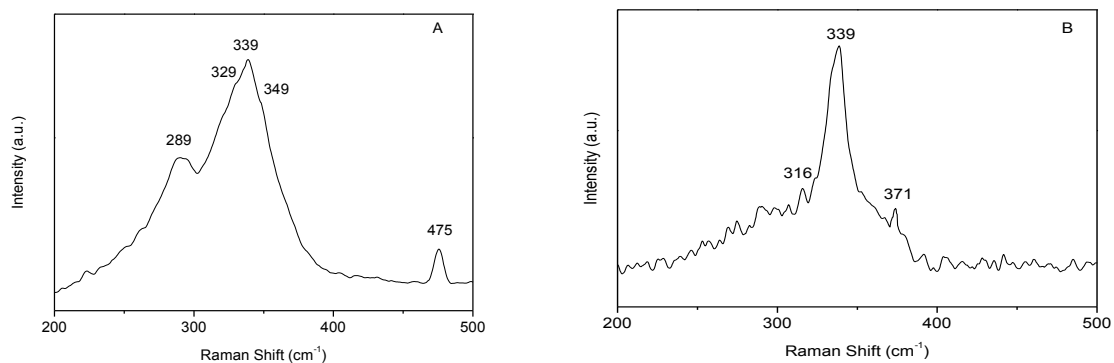


Fig. 3. Micro-Raman spectrum of spray deposited CZTS films with two tin precursors (A & B).

Figs. 4 and 5 shows scanning electron micrograph of as deposited CZTS films with two different tin precursors and films were annealed in sulphur environment. The surface morphology of as deposited CZTS films with solution A shows island like regions with slightly smeary appearance. The distinct grains were observed, in the films deposited with solution B. The annealing condition enhances the crystallinity of these films.

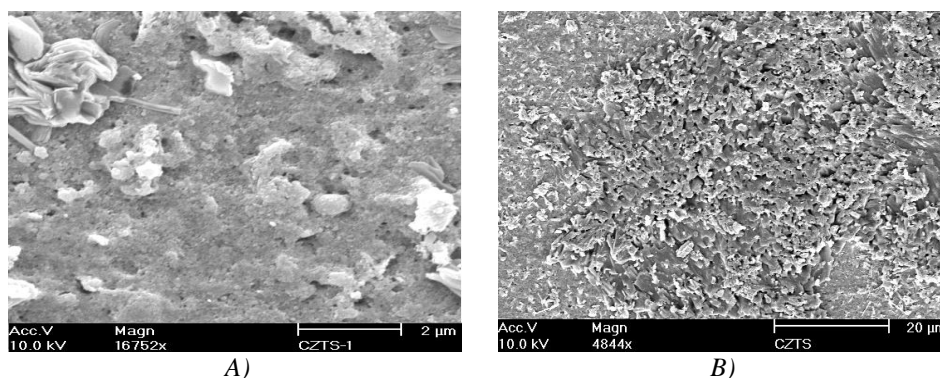


Fig. 4. SEM micrographs of spray deposited CZTS films with two tin precursors (A & B).

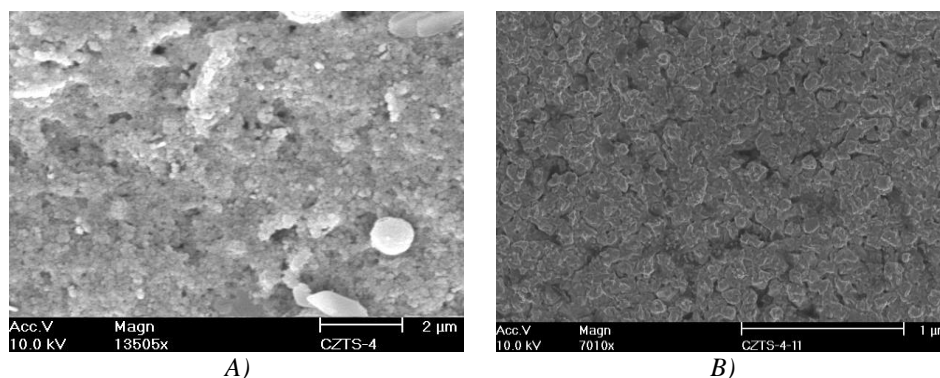


Fig. 5. SEM micrographs of CZTS films with two tin precursors (A & B) annealed at 760 K.

Fig. 6 shows the typical spectral transmittance (T) as a function of wavelength for the spray deposited CZTS film with precursor solution B. The sharp decrease of T near the fundamental absorption edge represent the optical transition is direct. The optical absorption

coefficient (α) of these films was determined using simple equation $\alpha = \frac{1}{t} \ln \left[\frac{(1-R)^2}{T} \right]$, where R is spectral reflectance and t is thickness of film [28, 29].

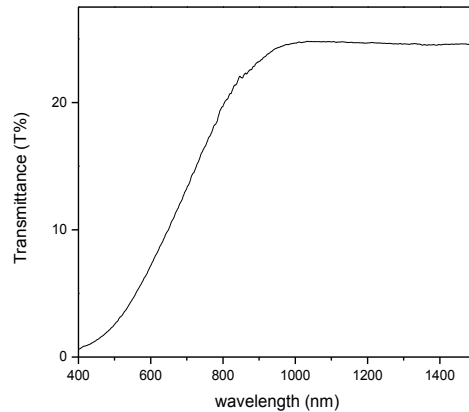


Fig. 6. Spectral transmittance of spray deposited CZTS films with solution B.

Fig. 7 shows the typical optical absorption coefficient as a function of photon energy ($h\nu$) of CZTS film with solution B. The magnitude of α of these films is determined to be $\geq 10^4 \text{ cm}^{-1}$. The direct optical transitions and absorption process is described by the simple relation $(\alpha h\nu) = a(h\nu - E_g)^{1/2}$, where a is constant [28, 29].

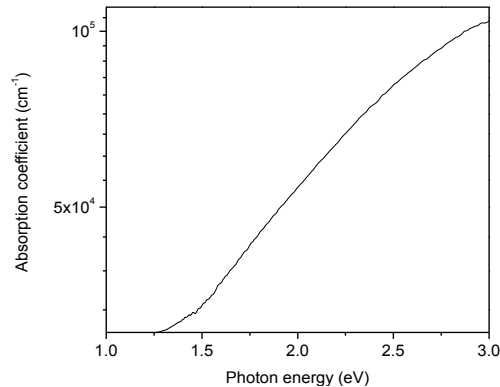


Fig. 7. Optical absorption coefficient of spray deposited CZTS film with solution B.

Fig. 8 shows the Tauc plot of CZTS thin films with solutions A and B. The band gaps of films obtained from the intercept on $h\nu$ -axis, were found to be 1.40 eV and 1.92 eV for solution A. The former band gap is attributed to CZTS and latter is assigned to Cu_{2-x}S [30]. The band gap of CZTS films obtained from solution B is found to be 1.48 eV. The relative ambiguity in the estimated the band gap is $\pm 0.02 \text{ eV}$. This band gap of CZTS films is concord with the optical band gap reported earlier [8, 16]. The obtained energy gap is close to ideal energy band gap of solar spectrum.

Films being rich in zinc, zinc sulphide might be there in the films. However, the presence of zinc sulphide could not recognize in the transmission spectrum of below 550 nm region after the intense absorption of CZTS phase in the sample. The band gap of annealed at 760 K are found to be $1.55 \pm 0.02 \text{ eV}$.

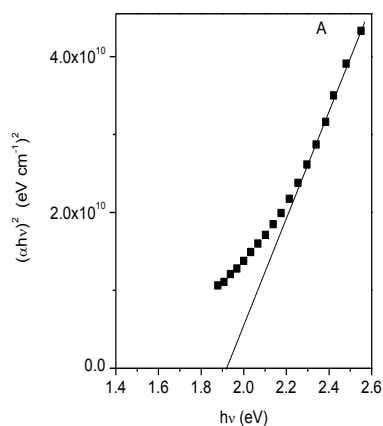


Fig. 8. a $(\alpha hv)^2$ as a function of photon energy ($h\nu$) of $Cu_{2-x}S$ films deposited with solution A.

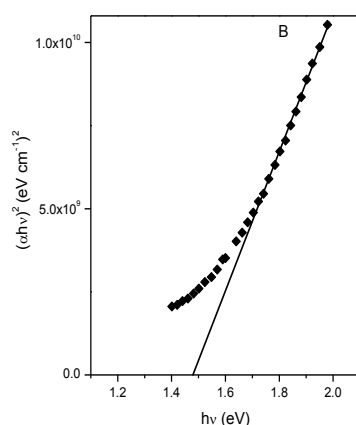


Fig. 8. b $(\alpha hv)^2$ as a function of photon energy ($h\nu$) of CZTS films deposited with solution B.

Van der Pauw technique was applied for room temperature electrical resistivity studies and were found to be 42 and 09 Ω -cm. The Hall mobility and carrier concentration of as deposited CZTS films were tabulated in Table 2. The obtained values are concord with reported values [24]. Using hot probe technique, the films were found to be exhibiting p-type nature.

Table 2. Room temperature electrical performances of CZTS films.

Sample Code	Condition	resistivity Ω -cm	carrier concentration cm^{-3}	Hall mobility Cm^2/Vs	Type of conductivity
A	As deposited	42	0.65×10^{17}	2.28	p-type
B	As deposited	09	0.36×10^{18}	2.50	p-type

An attempt was made to fabricate a typical Cu_2ZnSnS_4 solar cell by chemical techniques [20]. Cu_2ZnSnS_4 thin films were deposited using spray solution consisting of stannic chloride onto CdS films in the sequence glass/ZnO:Al/CdS/CZTS/Au. CdS thin films used as window layer were deposited by CBD technique at 340 K [31]. The thicknesses of the CZTS and CdS thin film layers were around 2.0 μm and 200 nm respectively. These layers were slightly heated at 470 K for about 20 minutes for the formation of metallurgical junction between CZTS/Cds thin films. The heterojunction thin film solar cell in the superstrate configuration was illuminated by a light source of intensity about 100 mW/cm^2 and the CZTS solar revealed an open circuit voltage (V_{oc}) and short circuit current (I_{sc}) of 126 mV and 1.2 mA/cm^2 . The obtained cell parameters are too

low. This might be due to the poor crystallinity and existence of secondary phases in the sample. In addition to these, low electrical mobility of CZTS films, recombination loss at the grain boundary surfaces and non-optimized respective film thickness might be the causes the poor device performance. As on today, maximum reported conversion efficiency of chemical spray deposited CZTS thin film solar cells is $< 2\%$ [16]. The efforts are under progress to attain a reasonable efficiency.

4. Conclusions

$\text{Cu}_2\text{ZnSnS}_4$ thin films have been successfully deposited with two tin precursors using chemical spray pyrolysis method. The number of grains per unit area were found to increase when the films were deposited with the aqueous solution containing stannic chloride. The structural, surface morphological, compositional, optical and electrical properties of these films were studied. XRD studies revealed that the films are polycrystalline in nature exhibiting kesterite structure. The lattice parameters of these films were found to be $a = b = 0.544$ nm and $c = 1.084$ nm. The optical band gap of the films is close to ideal energy gap and the absorption coefficient is above 10^4 cm^{-1} . The films exhibited p-type nature. An effort is made in this investigation to fabricate a typical heterojunction solar cell.

Acknowledgments

One of the authors Y.B. Kishore Kumar would like thank University Grants Commission (UGC), New Delhi, India for sanctioning a minor research project to carry out this research work.

References

- [1] T. M. Razykov, C. S. Ferekides, D. Morel, E. Stefanakos, H. S. Ullal, H. M. Upadhyaya, *Solar Energy* **85**(8), 1580 (2011).
- [2] J. Wu, Y. Hirai, T. Kato, H. Sugimoto, V. Bermudez, 7th World Conference on Photovoltaic Energy Conversion 10 (2018).
- [3] T. K. Todorov, K. B. Reuter, D. B. Mitzi, *Advanced Materials* **22**, 1 (2010).
- [4] K. Ito, T. Nakazawa, *Japanese Journal of Applied Physics* **27**(11), 2094 (1988).
- [5] Y. Chang, J. Huang, K. Sun, S. Johnston, Y. Zhang, H. Sun, A. Pu, M. He, et al., *Nature Energy* **3**, 764 (2018).
- [6] P. A. Fernandes, P. M. P. Salomé, A. F. da Cunha, Björn-Arvid Schubert, *Thin Solid Films* **519**, 7382 (2010).
- [7] K. Oishi, G. Saito, K. Ebina, M. Nagahashi, K. Jimbo, W. S. Maw, H. Katagiri, M. Yamazaki, H. Araki, A. Takeuchi, *Thin Solid Films* **517**, 1449 (2008).
- [8] H. Katagiri, K. Saitoh, T. Washio, H. Shinohara, T. Kurumadani, S. Miyajima, *Solar Energy Materials and Solar Cells* **65**, 141 (2001).
- [9] S. Tajima, M. Umehara, M. Hasegawa, T. Mise, T. Itoh, *Progress in Photovoltaics: Research and Applications* **25**(1), 14 (2017).
- [10] X. Jin, C. Yuan, G. Jiang, W. Liu, C. Zhu, *Materials Letters* **175**, 180 (2016).
- [11] P. K. Sarswat, M. L. Free, A. Tiwari, *Physica Status Solidi B* **248**(9), 2170 (2011).
- [12] R. Kabilan, T. P. Kumar, R. Suman, M. S. Revathy, T. Chitravel, R. Ravi, *Chalcogenide Letters* **16**(3), 137 (2019).
- [13] S. S. Mali, B. M. Patil, C. A. Betty, P. N. Bhosale, Y. W. Oh, S. R. Jadkar, R. S. Devan, Y. R. Ma, P. S. Patil, *Electrochimica Acta* **66**, 216 (2012).
- [14] B. Long, S. Cheng, Y. Lai, H. Zhou, J. Yu, Q. Zheng, *Thin Solid Films* **573**, 117 (2014).
- [15] A. Wangperawong, J. S. King, S. M. Herron, B. P. Tran, K. Pangan-Okimoto, S. F. Bent, *Thin Solid Films* **519**, 2488 (2011).
- [16] M. Courel, E. V. Resendiz, J. A. A-Arvizu, E. Saucedo, O. Vigil-Galán, *Solar Energy*

- Materials and Solar Cells **159**, 151 (2017).
- [17] N. Nakayama, K. Ito, Applied Surface Science **92**, 171 (1996).
- [18] V. M. Reddy, P. Mohan Reddy, G. P. Reddy, G. Sreedevi, K. K. Y. B. Reddy, P. Babu, W. K. Kim, K. T. R. Reddy, C. Park, Journal of Industrial and Engineering Chemistry **76**, 39 (2019).
- [19] Y. B. K. Kumar, G. S. Babu, P. U. Bhaskar, V. S. Raja, Physica Status Solidi A **206**(7), 1525 (2009).
- [20] Y. B. K. Kumar, V. S. Raja, Surfaces and Interfaces **9**, 233 (2017).
- [21] O. Vigil-Galán, M. E. Rodríguez, M. Courel, X. Fontané, D. Sylla, V. I. Roca, A. Fairbrother, E. Saucedo, A. P. Rodríguez, Solar Energy Materials and Solar Cells **117**, 246 (2013).
- [22] W. Schäfer, R. Nitsche, Materials Research Bulletin **9**, 645 (1974).
- [23] B. D. Cullity, Elements of X-Ray Diffraction, Addison Wesley, London (1978).
- [24] M. Courel, J. A. A. Arvizu, A. G. Cervantes, M. M. N. Marín, F. A. P. Agudelo, O. V. Galán, Materials and Design **114**, 515 (2017).
- [25] G. Sunny, T. Thomas, D. R. Deepu, C. S. Kartha, K. P. Vijayakumar, Optik **144**, 263 (2017).
- [26] P. A. Fernandes, P. M. P. Salomé, A. F. da Cunha, Journal of Alloys and Compounds **509**(28), 7600 (2011).
- [27] U. Chalapathi, Y. Jayasree, S. Uthanna, V. Sundara Raja, Physica Status Solidi A **210**(11), 2384 (2013).
- [28] I. V. Pankove, Optical processes in semiconductors, Dover Inc, New York (1975).
- [29] D. Nagamalleswari, Y. B. K. Kumar, Y. B. Kiran, G. S. Babu, Energy Sources, Part A: Recovery, Utilization and Environmental Effects **41**(24) 3001 (2019).
- [30] A. C. Rastogi, S. Salkalachen, Thin Solid Films **97**, 191 (1982).
- [31] T. Kamal, S. Parvez, K. M. Khabir, R. Matin, T. Hossain, H. Sarwar, M. S. Bashar, M. J. Rashid, South Asian Journal of Research in Engineering Science and Technology **2**(3), 610 (2017).